



# Polyethyleneimine-modified superparamagnetic Fe<sub>3</sub>O<sub>4</sub> nanoparticles: An efficient, reusable and water tolerance nanocatalyst

Mehdi Khoobi<sup>a</sup>, Tayebah Modiri Delshad<sup>b</sup>, Mohsen Vosooghi<sup>a</sup>, Masoumeh Alipour<sup>a</sup>, Hosein Hamadi<sup>c</sup>, Eskandar Alipour<sup>b</sup>, Majid Pirali Hamedani<sup>d</sup>, Seyed esmaeil Sadat ebrahimi<sup>a</sup>, Zahra Safaei<sup>b</sup>, Alireza Foroumadi<sup>a</sup>, Abbas Shafiee<sup>a,\*</sup>

<sup>a</sup> Department of Medicinal Chemistry, Faculty of Pharmacy and Pharmaceutical Sciences Research Center, Tehran University of Medical Sciences, Tehran 14176, Iran

<sup>b</sup> Department of Chemistry, Islamic Azad University, Tehran-North Branch, Zafar St., Tehran, Iran

<sup>c</sup> Department of Chemistry, College of Science, Shahid Chamran University, Ahvaz, Iran

<sup>d</sup> Iran Polymer & Petrochemical Institute, P.O. Box 14965/115, Tehran, Iran

## ARTICLE INFO

### Article history:

Received 20 May 2014

Received in revised form

30 August 2014

Accepted 17 September 2014

### Keywords:

Polyethyleneimine (PEI)

Magnetic Nanoparticle

Spiro-oxindole

Pyranol[3,2-c]chromene

Surface functionalization

## ABSTRACT

A novel magnetically separable catalyst was prepared based on surface modification of Fe<sub>3</sub>O<sub>4</sub> magnetic nanoparticle (MNPs) with polyethyleneimine (PEI) via covalent bonding. [3-(2,3-Epoxypropoxy)propyl] trimethoxysilane (EPO) was used as cross linker to bond PEI on the surface of MNPs with permanent stability in contrast to PEI coating via electrostatic interactions. The synthesized catalyst was characterized by Fourier transform infrared (FT-IR), thermogravimetric analysis (TGA), X-ray powder diffraction (XRD), transmission electron microscopy (TEM) and vibrating sample magnetometry (VSM). The catalyst show high efficiency for one-pot synthesis of 2-amino-3-cyano-4H-pyran derivatives via multi-component reaction (MCR). This procedure offers the advantages of green reaction media, high yield, short reaction time, easy purification of the products and simple recovery and reuse of the catalyst by simple magnetic decantation without significant loss of catalytic activity.

© 2014 Published by Elsevier B.V.

## 1. Introduction

The aim of green chemistry is to find alternative processes to conserve resources and reduce costs. Application of environmentally benign solvents instead of toxic and/or hazardous solvents and also utilizing of mild conditions and inexpensive reagents are the most fascinating strategies to develop a simple and green synthesis of organic compounds [1,2]. Water as an available and inexpensive solvent in large quantities can facilitate the rate of organic reactions even for water-insoluble reactants as well as product isolation by simple filtration. In addition, application of catalytic rather than stoichiometric reagents and reducing considerably the reaction times are important factors in order to

increase the environmental concerns [2]. Catalyst plays an important role in green chemistry as it can provide the best yield of the reaction in the reduced temperatures. Nanocatalysts as bridge between homogenous and heterogeneous catalysts can provide both benefits of them including high activity and selectivity as well as stability and ease of isolation or recovery. Considerable properties of magnetic nanoparticles (MNPs) such as large surface area to volume ratios, biocompatibility, non-toxicity and simple modification made them attractive for several biomedical applications [3]. In addition to all the mentioned features, easy and complete recovery of MNPs by means of an external magnet due to their superparamagnetic property makes them the best catalyst for green and sustainable chemistry. The surface of the MNPs has to protect by a suitable coating materials in order to protect their surface from oxidation, reduce the aggregating tendency and subsequently improve their dispersibility and colloidal stability [4–9].

PEI as a water soluble cationic polymer have been widely used in drug/gene delivery [10–12], CO<sub>2</sub> adsorption [13], nucleic acid precipitation, protein coagulation/flocculation [14], nucleotide, cell and enzyme immobilization [15–18]. It was found that PEI can stabilize nanoparticles as a capping and reducing agent [19]. Although, there are several reports about preparation and

Abbreviations: ; DLS, dynamic light scattering; EG, ethylene glycol; EPO, [3-(2,3-epoxypropoxy)propyl]trimethoxysilane; FT-IR, Fourier transform infrared; HD, hydrodynamic diameter; MCR, multi-component reaction; MNPs, magnetic nanoparticle; PG, propylene glycol; PEI, polyethyleneimine; TLC, thin layer chromatography; TGA, thermogravimetric analysis; TEM, transmission electron microscopy; VSM, vibrating sample magnetometry; XRD, X-ray powder diffraction; SEM, scanning electron microscopy

\* Corresponding author. Fax: +98 21 66461178.

E-mail address: [ashafiee@ams.ac.ir](mailto:ashafiee@ams.ac.ir) (A. Shafiee).

<http://dx.doi.org/10.1016/j.jmmm.2014.09.044>

0304-8853/© 2014 Published by Elsevier B.V.

application of PEI-functionalized MNPs, must of them are based on electrostatic adsorption of positively charged PEI on the negatively charged surface of MNPs [18]. Only a few reports could be found about application of PEI as a catalyst [23–28]. Amali et al. have reported Pd entrapped by highly branched PEI on the surface of  $\text{Fe}_3\text{O}_4$  as successful catalyst in hydrogenation and ligand-free Suzuki–Miyaura reactions [23]. Gold nanoparticles immobilized on PEI modified  $\text{Fe}_3\text{O}_4$  show good efficiency in reduction of 4-nitrophenol [24,27]. Layer-by-layer assembly via electrostatic interaction have been used to prepare PEI coated  $\text{Fe}_3\text{O}_4$  as catalyst in all reports.

4H-pyrans are well known as privileged scaffolds of the emerging drugs with numerous medicinal activities and show diverse applications in laser dyes, pigments, cosmetics, optical fluorescence markers and brighteners [28]. Bearing in mind the efficiency of PEI as a water soluble catalyst and in connection with our previous works [29], we decided to explore novel PEI covalently bound on the surface of MNPs by [3-(2,3-epoxypropoxy)propyl]trimethoxysilane (EPO) as cross linker (PEI@Si-MNPs) for the preparation of chromene (4), pyrano[3]chromene (6), and spiro-oxindole (9,11) derivatives (see Scheme 1).

## 2. Experimental

### 2.1. General

[3-(2,3-Epoxypropoxy)propyl]trimethoxysilane (EPO, 98% purity), aqueous ammonia solution (28 wt%), ferric chloride hexahydrate ( $\text{FeCl}_3 \cdot 6\text{H}_2\text{O}$ ), and ferrous chloride tetrahydrate ( $\text{FeCl}_2 \cdot 4\text{H}_2\text{O}$ ) were purchased from Merck (Darmstadt, Germany). Hyperbranched PEI (Mw=60,000) were purchased from Sigma-Aldrich (St. Louis, MO, USA). X-ray diffraction (XRD) patterns were recorded with a XPert MPD advanced diffractometer. The magnetic properties of the samples were detected at room temperature using a vibrating sample magnetometer (VSM, Meghnatis Kavir Kashan Co., Kashan, Iran). The particle

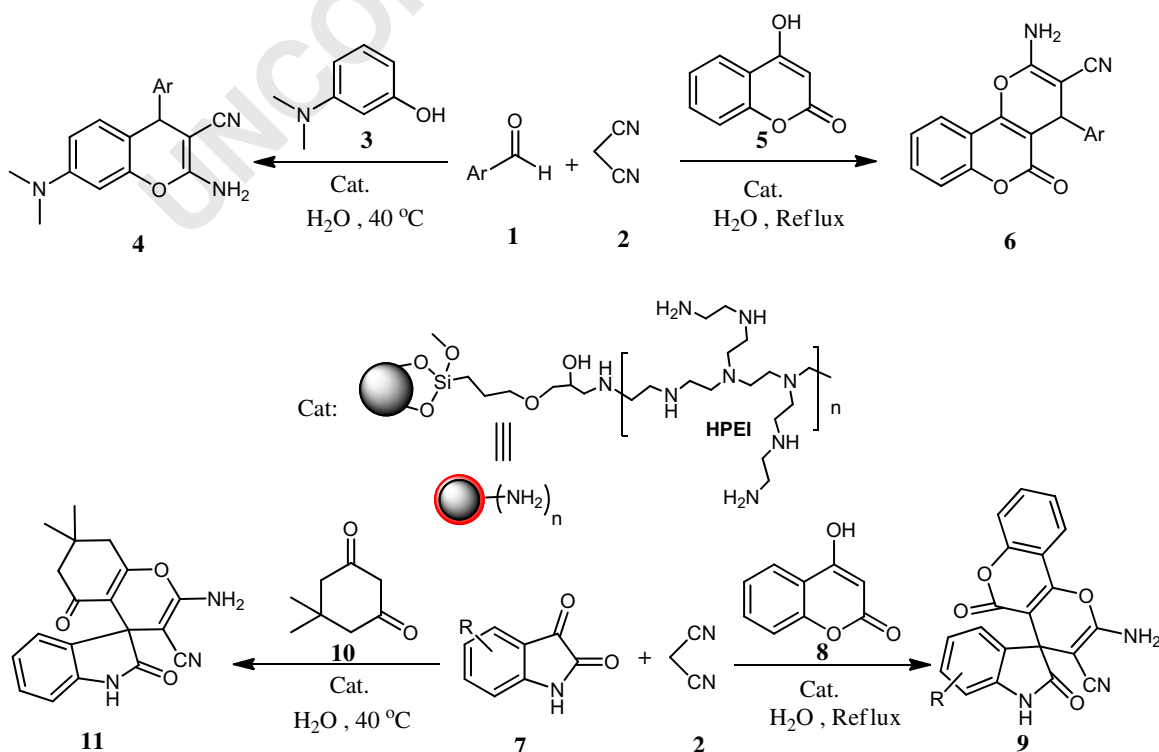
size and morphology of the sample surfaces were analyzed by scanning electron microscopy (VEGAII TESCAN) with an acceleration voltage of 15 kV. The disk was pasted with copper tape, and the sample was dispersed over the tape. The disk was coated with gold in an ionization chamber. Transmission electron microscopy (TEM) was carried out on EM208 Philips. Samples were prepared by placing a droplet (1  $\mu\text{L}$ ) of nanocomposite dispersion latex, along with a droplet of water, on a copper grid covered by Formvar foil (200 mesh). FT-IR spectra were obtained using Nicolet FT-IR Magna 550 spectrographs (KBr disks) spectrometer. Melting points were measured on a Kofler hot stage apparatus and are uncorrected. NMR spectra were recorded in  $\text{CDCl}_3$  on a Bruker 500 MHz spectrometer.

### 2.2. Synthesis of PEI@Si-MNPs

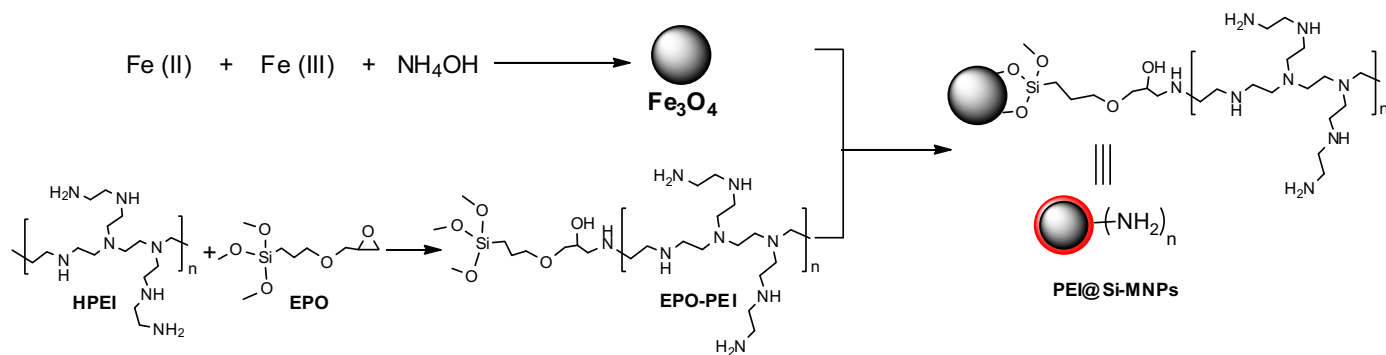
$\text{Fe}_3\text{O}_4$  MNPs were synthesized using the chemical coprecipitation method [30]. In order to graft PEI onto  $\text{Fe}_3\text{O}_4$  MNPs, EPO (1 mmol) was added to a stirred solution of 150 mL dry toluene containing 1.5 g of PEI. The resultant mixture was allowed to react at 80 °C for 24 h. To this solution, 2.5 g of  $\text{Fe}_3\text{O}_4$  MNPs and 25 mL of ethanol were added, and the solution was stirred at 80 °C for 24 h. PEI@Si-MNPs was magnetically isolated by an external magnet and repeatedly washed with ethanol (Scheme 2). Subsequently, it was washed repeatedly with water and ethanol to remove unreacted substrates and byproducts, and dried at 40 °C for several days [24].

### 2.3. General procedure for catalytic synthesis of compounds 4, 6, 9, 11

A stirring mixture of an active carbonyl compound (aldehyde 1 or isatin 7, 1 mmol), malononitrile 2 (1.2 mmol), magnetic catalytic system ([PEI@Si-MNPs], 5 mg) and ethylene glycol/water (EG/ $\text{H}_2\text{O}$  20/80, 2 mL) were sonicated for one minute. To this stirred mixture, an enolizable compounds (3-(dimethylamino)phenol 3, 4-hydroxycoumarin 5 or dimedone 10, 1 mmol) was added. The



Scheme 1. PEI@Si-MNPs catalyzed one-pot synthesis of various 4H-pyrans.



Scheme 2. Schematic representation of the formation of PEI@Si-MNPs.

Table 1

Optimization of reaction conditions for three-component reaction of benzaldehyde, malononitrile and 4-hydroxycoumarin or 3-(dimethylamino)phenol.

Entry	Catalyst	Solvent	Cat. (mg)	T (°C)	Time (h)	Yield (%) <sup>a</sup>
1	–	H <sub>2</sub> O	–	100	10	21
2	Fe <sub>3</sub> O <sub>4</sub> MNPs	H <sub>2</sub> O	5	100	2	45
3	PEI	H <sub>2</sub> O	5	100	2	62
4	PEI@Si-MNPs	H <sub>2</sub> O	5	rt	5	52
5	PEI@Si-MNPs	H <sub>2</sub> O	5	100	1	82
6	PEI@Si-MNPs	–	5	100	1	72
7	PEI@Si-MNPs	Propylene glycol (PG)	5	100	1	85
8	PEI@Si-MNPs	Ethylene glycol (EG)	5	100	1.5	89
9	PEI@Si-MNPs	EG/H <sub>2</sub> O (50/50)	5	100	1	88
10	PEI@Si-MNPs	EG/H <sub>2</sub> O (80/20)	5	100	1	85
11	PEI@Si-MNPs	EG/H <sub>2</sub> O (20/80)	5	100	1	98
12	–	EG/H <sub>2</sub> O (20/80)	–	100	2	72
13 <sup>b</sup>	PEI@Si-MNPs	EG/H <sub>2</sub> O (20/80)	5	rt	1	70
14 <sup>b</sup>	PEI@Si-MNPs	EG/H <sub>2</sub> O (20/80)	5	40	1.5	94
15	PEI@Si-MNPs	EtOH	5	78	1	70
16	PEI@Si-MNPs	CH <sub>3</sub> CN	5	60	1	45

Reaction conditions: 4-hydroxycoumarin (1 mmol), malononitrile (1.2 equiv.), benzaldehyde (1.2 equiv.), solvent (2 mL) and the required amount of catalyst.

<sup>a</sup> The yields refer to the isolated product.<sup>b</sup> Reaction of 3-(dimethylamino) phenol (1 mmol), malononitrile (1.2 equiv.), 4-nitro benzaldehyde (1.2 equiv.), solvent (2 mL) and the required amount of catalyst.

Table 2

Results of three-component reaction of 4-hydroxycoumarin, malononitrile and different aldehydes catalyzed by PEI@Si-MNP in EG/H<sub>2</sub>O.

Entry	Product	Yield <sup>a</sup>	Time (min)	m.p. <sup>b</sup> (°C)	Entry	Product	Yield <sup>a</sup>	Time (min)	m.p. (°C)
1		94	60	> 250	4		91	60	221–223
2		20	10 h <sup>c</sup>	> 250	5		89	55	> 250
3		96	50	> 250	6		81	70	> 250

<sup>a</sup> Isolated yield.<sup>b</sup> Similar to the literatures m.p. [30–35].<sup>c</sup> No catalyst, H<sub>2</sub>O, reflux, 10 h.

**Table 3**Results of three-component reaction of 3-(dimethylamino)phenol, malononitrile and different aldehydes catalyzed by PEI@Si-MNPs in EG/H<sub>2</sub>O.

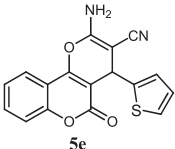
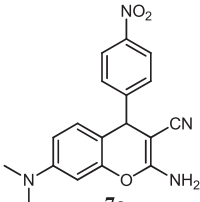
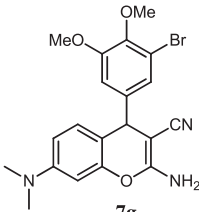
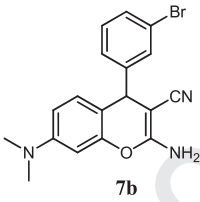
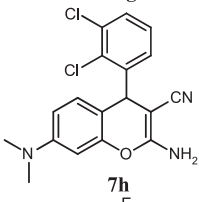
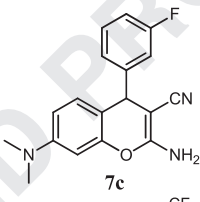
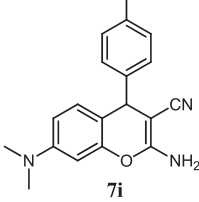
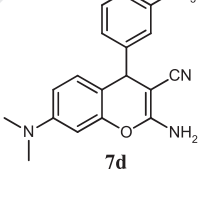
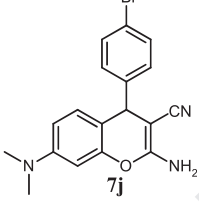
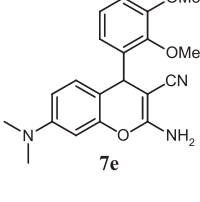
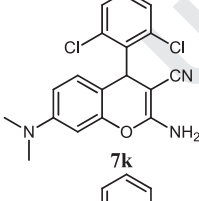
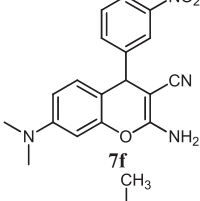
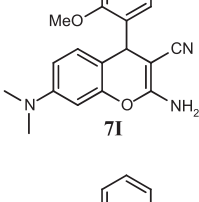
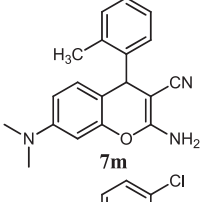
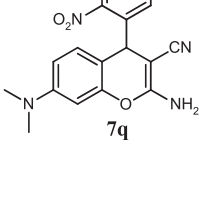
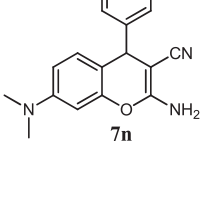
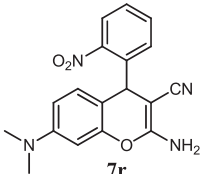
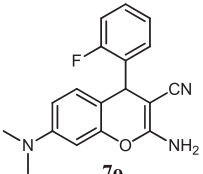
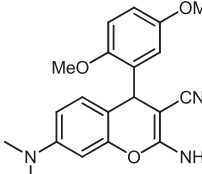
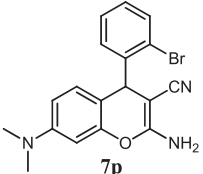
Entry	Product	Yield <sup>a</sup>	Time (min)	m.p. <sup>b</sup>	Entry	Product	Yield <sup>a</sup>	Time (min)	m.p. <sup>b</sup> (°C)
1		94	90	224–226	7		81	100	204–206
2		91	90	194–196	8		85	90	220–222
3		88	100	163–166	9		87	80	174–178
4		92	80	214–218	10		89	80	212–214
5		86	100	158–160	11		83	100	> 250
6		93	90	207–209	12		82	100	182–184
13		89	80	155–157	17		81	90	192–194
14		90	90	161–163	18		86	100	142–144
15		85	80	209–211	19		81	120	162–164

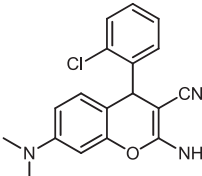
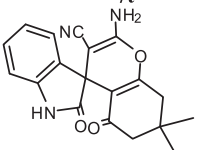
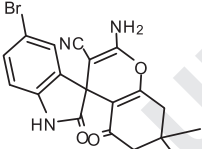
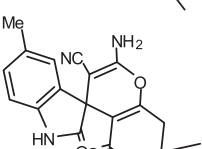
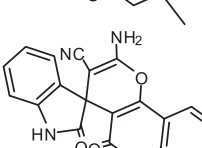
Table 3 (continued)

Entry	Product	Yield <sup>a</sup>	Time (min)	m.p. <sup>b</sup>	Entry	Product	Yield <sup>a</sup>	Time (min)	m.p. <sup>b</sup> (°C)
16		81	100	201–203	20		78	100	195–197
									

<sup>a</sup> Isolated yield.<sup>b</sup> Similar to the literatures m.p. [30–35].

Table 4

Results of three-component synthesis of spirooxindole derivatives **9** using isatin, malononitrile and dimedone and **11** using isatin, malononitrile and 4-hydroxycoumarin by PEI@Si-MNP in EG/H<sub>2</sub>O

Entry	Product	Yield <sup>a</sup>	Time (min)	m.p. <sup>b</sup>
1		97	30	> 250
2		95	30	> 250
3		95	40	> 250
4		97	45	> 250
5		92	30	> 250

<sup>a</sup> Isolated yield.<sup>b</sup> Similar to the literatures m.p. [33].

reaction mixture was heated at appropriate temperature as mentioned in Table 1. The progress of the reaction was monitored by TLC. After completion of the reaction (as shown in Tables 2–4), the

reaction mixture was allowed to cool at room temperature and diluted with ethyl acetate and the catalyst was easily separated from the reaction mixture with an external magnet and washed twice with ethyl acetate. The combined organic layers were concentrated in vacuum and the residue was purified by crystallization from ethanol. All compounds gave satisfactory spectral data and they were identical with those reported in the literature [29,31–37].

### 3. Results and discussion

As illustrated in Scheme 2, the catalyst was prepared easily by two step process. Initially, the amine groups of PEI reacted with epoxy group of EPO, and then the latter was covalently anchored on the surface of MNPs through reaction of trimethoxysilane groups of EPO-PEI with hydroxyl groups of MNPs via a silanization reaction.

#### 3.1. Chemical-physical characterization of PEI@Si-MNPs

##### 3.1.1. FT-IR

The as-synthesized PEI@Si-MNPs catalyst was characterized by various techniques. The FT-IR spectrum of PEI@Si-MNPs, shows bands at 1581 and 1457 cm<sup>-1</sup> assigned to the stretching vibration of C–N and bending vibration of C–H bonds of PEI macromolecular chains respectively, which are chemically linked on the surfaces of MNPs and the bands at around 2924 and 2831 cm<sup>-1</sup> are attributed to stretching vibration of the aliphatic C–H bands. In addition, the characteristic peaks of Fe–O at 584 cm<sup>-1</sup> and strong adsorption band at 1029–1023 cm<sup>-1</sup> of Si–O–Si and Si–OH were also observed (Fig. 1).

##### 3.1.2. XRD

The X-ray diffraction patterns of MNPs and PEI@Si-MNPs are shown in Fig. 2. The position and relative intensity of all the diffraction peaks suitably matched those of standard Fe<sub>3</sub>O<sub>4</sub> [38]. The MNPs are in the form of inverse spinel Fe<sub>3</sub>O<sub>4</sub> with a face-centered cubic structure, suggesting that the sample has a cubic crystal system. Moreover, no characteristic peaks of impurities were observed in the XRD spectrum. The comparison of the diffraction patterns of MNPs and PEI@Si-MNPs shows that the broadening of these diffraction peaks is reflective of polycrystalline as-prepared MNPs. The Bragg diffraction angles are nearly



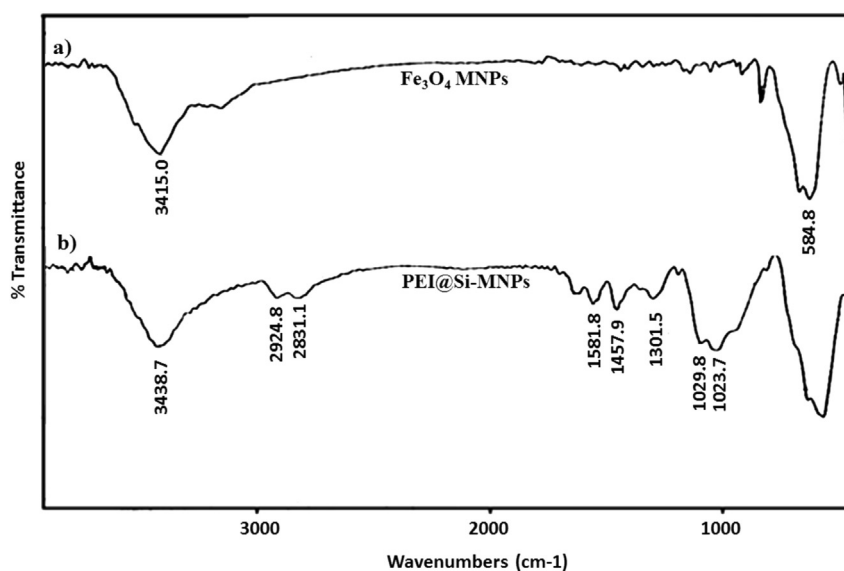


Fig.1. FT-IR spectrum of  $\text{Fe}_3\text{O}_4$  MNPs and PEI@Si-MNPs.

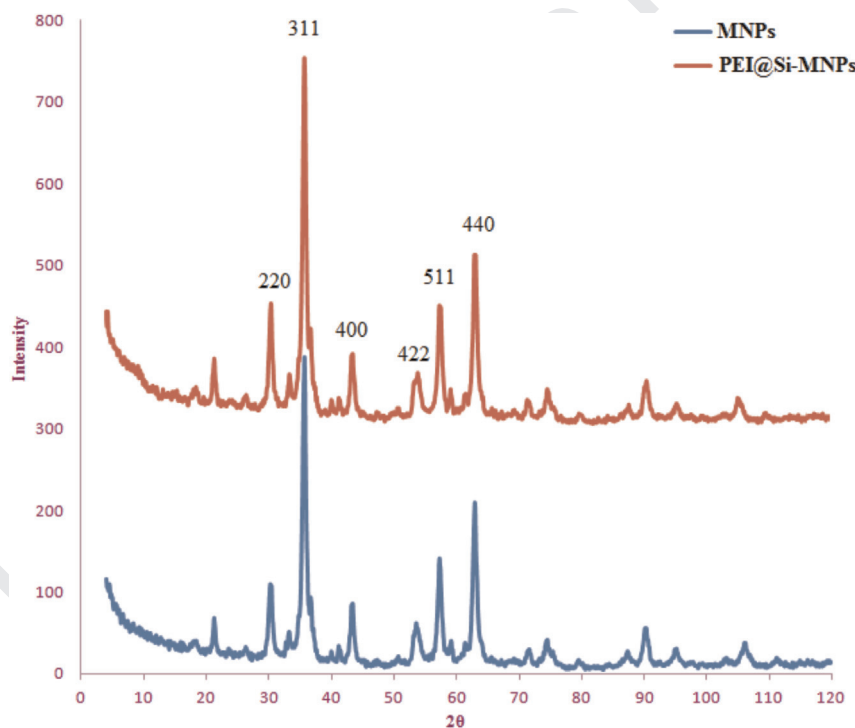


Fig. 2. XRD patterns of  $\text{Fe}_3\text{O}_4$  MNPs and PEI@Si-MNPs.

identical, indicating that the structures of the MNPs are preserved after PEI coating. The average crystallite sizes of MNPs were estimated 17.2 nm using Scherrer's equation.

### 3.1.3. TGA

TGA curves of  $\text{Fe}_3\text{O}_4$  MNPs and PEI@Si-MNPs are shown in Fig. 3a. Three steps of weight loss are found in the thermogram of MNPs. The first weight loss of about 1% at the range of 25–150 °C could be attributed to the desorption of hydrogen bonded water molecule, and the second weight loss of approximately 0.5% at 150–300 °C may be due to the removal of trapped water molecules

from the lattice. Final weight loss of 0.8% is appeared at the range 300–800 °C which is due to the phase transition of  $\text{Fe}_3\text{O}_4$  to FeO which is thermodynamically stable above 570 °C in phase diagram of the Fe–O system [39]. Rahman et al. [39] were also exhibited two steps of weight loss including 0.4%, 2% and 2.1% at temperature ranges of 25–150 °C, 150–300 °C and 650–800 °C, respectively. Thermogram of MNPs@PEI was also show three steps of weight loss attributed to the 5% weight loss in the temperature range of 50–150 °C relating to the vaporization of water, followed by 20% weight loss at the temperature range of 150–500 °C, which could be ascribed to oxidative decomposition of organic moiety. In the final step, the weight loss (5% at the temperature range of

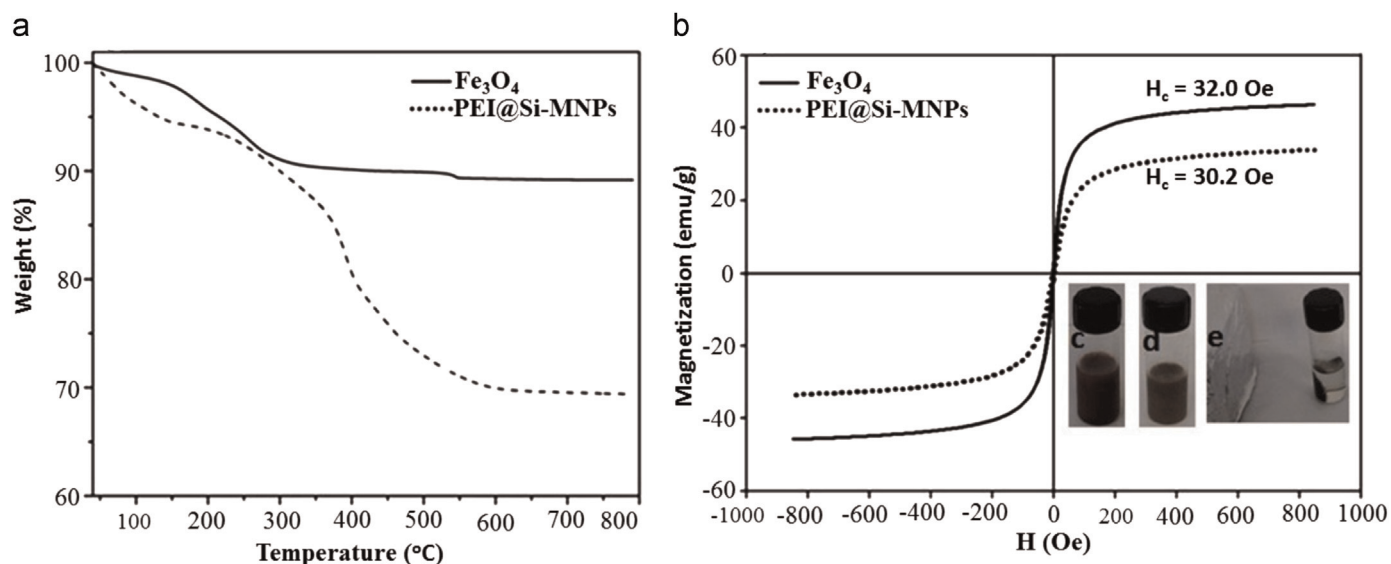


**Fig. 3.** (a) TGA of  $\text{Fe}_3\text{O}_4$  MNPs and PEI@Si-MNPs; (b) hysteresis loops of MNPs and PEI@Si-MNPs; (c–e) visible color change from red to gray during spiro-oxindole preparation and catalyst ability to effective recovery at the end of reactions. (For interpretation of the references to color in this figure legend, the reader is referred to the web version of this article.)

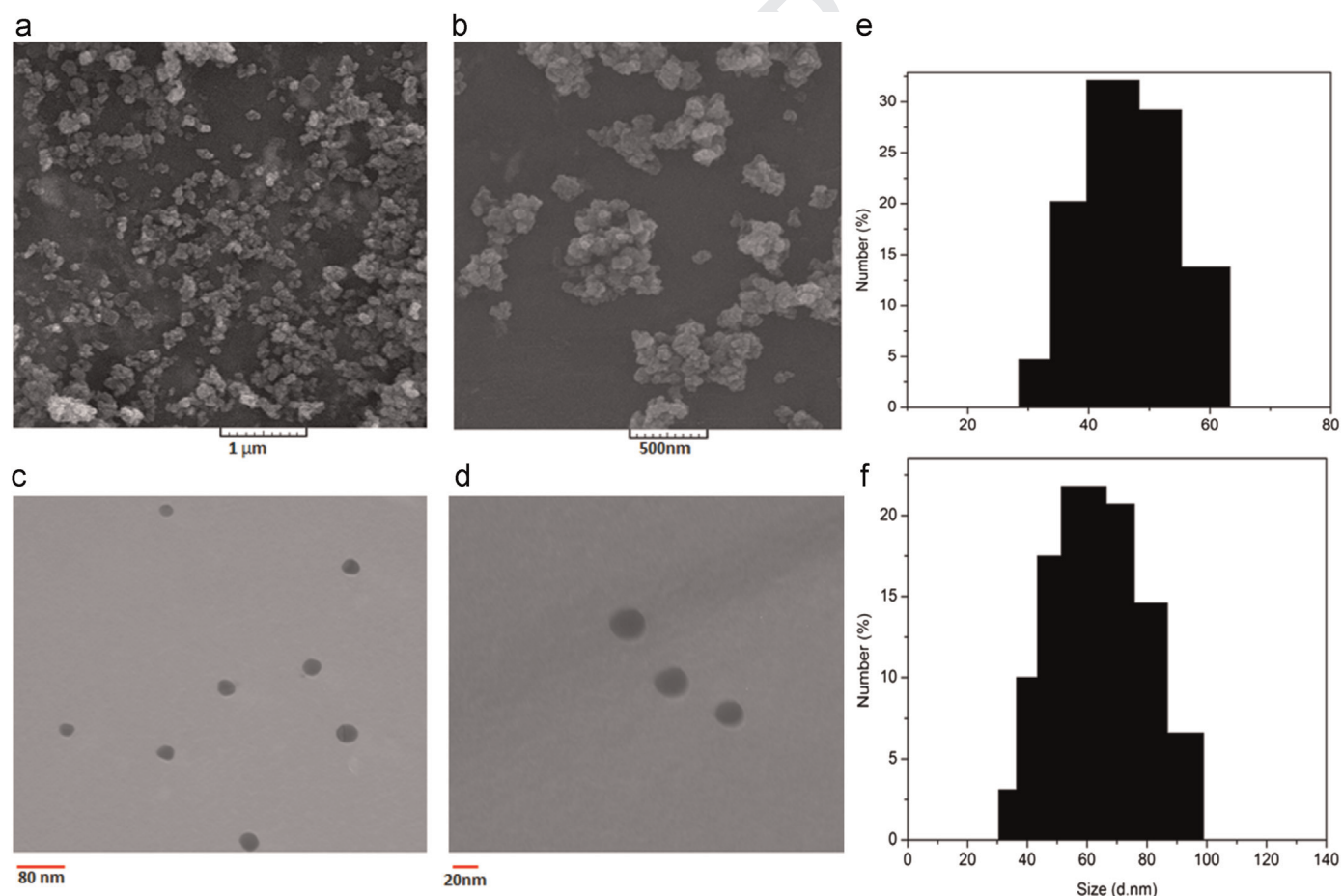


**Fig. 4.** SEM image of (a)  $\text{Fe}_3\text{O}_4$  MNPs, (b) PEI@Si-MNPs and (c, d) TEM image of PEI@Si-MNPs. (e) HDs sizes of  $\text{Fe}_3\text{O}_4$  MNPs and (f) PEI@Si-MNPs.

400–800 °C) could be ascribed to the phase transition of  $\text{Fe}_3\text{O}_4$  to FeO. From the percentage of weight loss in the TGA curve, the weight loss of MNPs@PEI nanoparticles was 30%. Comparison between the TGA results of  $\text{Fe}_3\text{O}_4$  MNPs and PEI@Si-MNPs show the percentage of EPO and PEI grafting density is about 20%.

### 3.2. Magnetic measurements

#### 3.2.1. VSM

Magnetic measurements for  $\text{Fe}_3\text{O}_4$  MNPs and PEI@Si-MNPs were performed using a vibrating sample magnetometer (VSM)

with a peak field of 8 kOe and their hysteresis curves are presented in Fig. 3b. It could be seen from the loops in Fig. 3b that the specific saturation magnetization ( $\sigma_s$ ) and the coercive field ( $H_c$ ), which represents the force required to rotate the magnetization vector of a magnet out of its equilibrium direction, for the  $\text{Fe}_3\text{O}_4$  MNPs are  $46.4 \text{ emu g}^{-1}$  and 32 Oe, respectively and those for PEI@Si-MNPs are 30.2 Oe and  $33.8 \text{ emu g}^{-1}$ , respectively. The decrease in mass saturation magnetization can be ascribed to the contribution of the non-magnetic silica and PEI shell. Although the  $\sigma_s$  values of the PEI@Si-MNPs have decreased; they still could be efficiently separated from solution with a permanent magnet. Fig. 3c–e shows the ability of the catalyst to effective recovery at the end of reactions.

### 3.3. Size and shape

#### 3.3.1. SEM and TEM

The SEM and TEM images of MNPs and PEI@Si-MNPs are presented in Fig. 4a–d. They show that most of the particles have quasi-spherical shape with the average size between 15 and 25 nm and they present uniform particles. These results are in good agreement with the XRD analysis (Fig. 2).

### 3.4. Colloidal

#### 3.4.1. DLS measurements

The hydrodynamic diameter (HD) sizes of  $\text{Fe}_3\text{O}_4$  MNPs and PEI@Si-MNPs were obtained in the range of 30–65 and 40–100 nm, respectively (shown in Fig. 4e and f). This increase in HD size of aqueous dispersion of MNPs@PEI could be attributed to coated silica and polymer layers.

### 3.5. Catalytic synthesis of 2-amino-3-cyano-4H-pyran derivatives

The catalytic activity of PEI@Si-MNPs was investigated for the synthesis of different 2-amino-3-cyano-4H-pyran derivatives using a MCR approach. For a model reaction, the reaction between benzaldehyde, malononitrile, and 4-hydroxycoumarin was chosen in the presence of innocuous solvents (Table 1). The catalytic performances of  $\text{Fe}_3\text{O}_4$  MNPs, PEI and PEI@Si-MNPs were screened in water using 5 mg of catalyst (Table 1, entries 2–5). Without the catalyst, the product was detected in 21% yields after 10 h (Table 1, entry 1).  $\text{Fe}_3\text{O}_4$  MNPs and PEI in bare form produced the product with 45 and 62% yields, respectively (Table 1, entries 2 and 3). Yet, their analogous combination in the form of PEI@Si-MNPs increased the yield up to 82% in a shorter reaction time (Table 1, entry 5). We then tried to screen the efficiency of the catalyst in different solvents in order to optimize the reaction conditions. A good result was obtained under neat conditions (Table 1, entry 6). But, the mixture was viscous without solvent and well dispersion and magnetically separation of the catalyst was difficult. Slightly higher yields were obtained when propylene glycol (PG) or ethylene glycol (EG) were used as the solvent instead of water (Table 1, entries 7 and 8). We noticed also that reducing in the quantity of the catalyst (5 mg) decreased the efficiency of the reaction and no meaningful difference was obtained when the catalyst increased slightly (data not shown). Interestingly, the reaction takes place in high yield without catalyst in the presence of EG/water (20/80) as solvent (72%, Table 1, entry 12). But the best result was obtained in EG/water (20/80) by 5 mg of the catalyst in a shorter reaction time (98%, Table 1, entry 11). The corresponding product was also obtained in 70% and 45% yields for ethanol and acetonitrile as the solvent, respectively (Table 1, entries 15 and 16). These results confirmed the crucial role of solvent in the dispersion of the nanocatalyst and adsorption of reactants on the surface

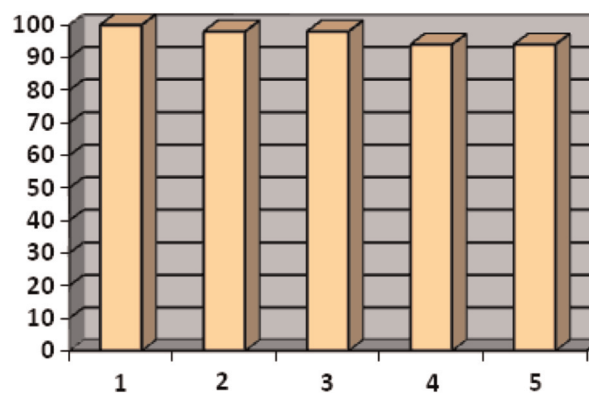


Fig. 5. Catalyst recycling experiments.

of the nanocatalyst which cause to increase the local concentration of reactants around the active sites of the catalyst.

With this result in hand, same procedure was used for the preparation of chromene derivatives **4** in excellent yields by means of three-component reactions of 3-(dimethylamino) phenol, malononitrile, and aldehyde catalyzed by mentioned magnetic catalytic system in EG/water at 40 °C and very short reaction times (Table 1, entry 14).

In order to explore the scope and the limitations of this catalytic method, we investigated various aldehydes containing either electron withdrawing or electron donating functional groups under the optimized reaction conditions. The results given in Tables 2 and 3 show that this one pot, three component condensation completed within 50–120 min, with good isolated yields. The results clearly indicate that reactions can tolerate a wide range of differently substituted aldehydes. In addition, it was observed that the reaction of 4-hydroxycoumarin was completed under reflux condition while the 3-(dimethylamino) phenol react at 40 °C.

In continuation to this research, a simple and an efficient one pot synthetic approach was used for the preparation of biologically interesting spirooxindole derivatives by means of three-component reactions of isatin, malononitrile, and dimedone or 4-hydroxycoumarin catalyzed by mentioned magnetic catalytic system in water (Table 4). Both dimedone and 4-hydroxycoumarin could give the product in excellent yields (92–97%). We noticed that using of 4-hydroxycoumarin need reflux condition to complete in relative short time while the dimedone react at 40 °C.

### 3.6. Catalyst recycling

To evaluate the stability and level of reusability of the catalyst, we decanted the vessel by use of an external magnet and the left used catalyst was washed with ethanol several times to remove residual product, dried under vacuum and reused in a subsequent reaction. A new reaction was then conducted with fresh reactants under similar conditions. It was found that the developed catalyst could be used at least five times and the conversion stayed with no detectable loss, more than 90% (see Fig. 5). Moreover, the FT-IR spectrum of the recovered catalyst showed no change after using it for five times. This indicates that no leaching of the PEI species occurred from support on using and reusing the catalyst.

## 4. Conclusions

In summary, we showed that PEI grafted on silica coated  $\text{Fe}_3\text{O}_4$  nanoparticles fabricated by covalently anchoring, was a novel and effective heterogeneous catalyst for the one-pot synthesis



of pyrano[3,2-c]chromene, chromenes and spiro-oxindoles derivatives from commercially available starting materials. The present method requires remarkably small amounts of non-toxic and environmentally friendly  $\text{PEI@Si-NMP}$  as catalyst. In addition the aqueous conditions, excellent yields, operational simplicity, practicability, product purity, cost efficiency and environmentally benefits are the worthy advantages of this protocol. The introduced magnetically nanocatalyst was highly stable and could be reused in 5 successive runs with no significant structural change and loss of activity.

Based on these observations, it could be concluded that this green and cost-effective catalyst, with simple experimental and work-up procedure, which avoids the use of large volumes of hazardous organic solvents, makes it a useful alternative for the scale-up of these three component reactions.

## Q2 Uncited references

[20–22].

## Acknowledgment

Q5 This work was supported by grants from the research council of Tehran University of Medical Sciences and Health Services and Q7 from the Iran National Science Foundation (INSF).

## Appendix A. Supplementary information

Supplementary data associated with this article can be found in the online version at <http://dx.doi.org/10.1016/j.jmmm.2014.09.044>.

## References

- [1] T. Erdmenger, C. Guerrero-Sanchez, J. Vitz, R. Hoogenboom, U.S. Schubert, *Chem. Soc. Rev.* 39 (2010) 3317–3333.
- [2] M. Abd El Aleem, A.A. El-Remaily, *Tetrahedron* 70 (2014) 2971–2975.
- [3] M. Mahmoudi, Sh. Sant, B. Wang, S. Laurent, T. Sen, *Adv. Drug Deliv. Rev.* 63 (2011) 24–46.
- [4] L. Lou, K. Yu, Z. Zhang, R. Huang, Y. Wang, Z. Zhu, *Appl. Surf. Sci.* 258 (2012) 8521–8526.
- [5] R.B.N. Baig, R.S. Varma, *Chem. Commun.* 49 (2013) 752–770.
- [6] F. Rajabi, N. Karimi, M.R. Saidi, A. Primo, R.S. Varma, R. Luque, *Adv. Synth. Catal.* 354 (2012) 1707–1711.
- [7] A. Kotarba, W. Bieniasz, P. Kustrowski, K. Stadnicka, Z. Sojka, *Appl. Catal. A* 407 (2011) 100–105.
- [8] M.L. Kantam, J. Yadav, S. Laha, P. Srinivas, B. Sreedhar, F. Figueras, *J. Org. Chem.* 74 (2009) 4608–4611.
- [9] A. Saha, J. Leazer, R.S. Varma, *Green Chem.* 14 (2012) 67–71.
- [10] C. Rudolph, J. Lausier, S. Naundorf, R.H. Müller, J. Rosenecker, *J. Gene Med.* 4 (2000) 269–278.
- [11] B. Chertok, A.E. David, V.C. Yang, *Biomaterials* 31 (2010) 6317–6324.
- [12] A. Barnard, P. Posocco, S. Pricl, M. Calderon, R. Haag, M.E. Hwang, V.W.T. Shum, D.W. Pack, D.K. Smith, J. Amr., *Chem. Soc.* 133 (2011) 20288–20300.
- [13] S. Satyapal, T. Filburn, J. Trela, J. Strange, *Energy Fuels* 15 (2001) 250–255.
- [14] J.J. Karimpil, J.S. Melo, S.F. D'Souza, *Int. J. Biol. Macromol.* 50 (2012) 300–302.
- [15] C.T. Chen, L.Y. Wang, Y.P. Ho, *Anal. Bioanal. Chem.* 399 (2011) 2795–2806.
- [16] W.-J. Song, J.-Z. Du, T.-M. Sun, P.-Z. Zhang, J. Wang, *Small* 6 (2010) 239–246.
- [17] H.J. Lee, S.G. Lee, E.J. Oh, H.Y. Chung, S.I. Han, E.J. Kim, S.Y. Seo, H.D. Ghim, J. H. Yeum, J.H. Choi, *Colloid Surf. B. Biointerfaces* 88 (2011) 505–511.
- [18] X. Wang, L. Zhou, Y. Ma, X. Li, H. Gu, *Nano Res.* 2 (2009) 365–372.
- [19] (a) K.R. Knowles, C.C. Hanson, A.L. Fogel, B. Warhol, D.A. Rider., *Appl. Mater. Interfaces* 4 (7) (2012) 3575–3583;
- (b) P.-L. Kuo, W.-F. Chen, H.-Y. Huang, I.-C. Chang, S.A. Dai, *J. Phys. Chem. B* 110 (7) (2006) 3071–3077.
- [20] S.C. McBain, H.H.P. Yiu, A.E. Haj, J. Dobson, *J. Mater. Chem.* 17 (2007) 2561–2565.
- [21] S. Huth, J. Lausier, S.W. Gersting, C. Rudolph, C. Plank, U. Welsch, J. Rosenecker, *J. Gene Med.* 6 (2004) 923–936.
- [22] Ch. W. Lim, I.S. Lee, *Nano Today* 5 (2010) 412–434.
- [23] A.J. Amali, R.K. Rana, *Green Chem.* 11 (2009) 1781–1786.
- [24] a) S.M. Ribeiro, A.C. Serra, A.M. d'A. Rocha Gonsalves, *Appl. Catal. A* 399 (2011) 126–133;
- b) P. Veerakumara, M. Velayudham, K.-L. Lu, S. Rajagopal, *Appl. Catal. A* 445 (2013) 247–260.
- [25] a) G.P. Royer, W.-Sh. Chow, K.S. Hatton, *J. Mol. Catal.* 31 (1985) 1–13;
- b) Z. Shen, Y. Chen, H. Frey, S.-E. Stiriba, *Macromolecules* 39 (2006) 2092–2099.
- [26] Y. Chi, S.T. Scroggins, E. Boz, J.M.J. Fre'chet, *J. Am. Chem. Soc.* 130 (2008) 17287–17289.
- [27] a) M.-L. Wang, T.-T. Jiang, Y. Lu, H.-J. Liu, Y. Chen, *J. Mater. Chem. A* 1 (2013) 5923–5933;
- b) H. Li, Sh. Gao, Zh. Zheng, R. Cao, *Catal. Sci. Technol.* 1 (2011) 1194–1201.
- [28] a) M.G. Dekamin, M. Eslami, A. Maleki, *Tetrahedron* 69 (2013) 1074–1085;
- b) Y. Gao, W. Yang, D.M. Du, *Tetrahedron: Asymmetry* 23 (2012) 339–344;
- c) G.A. Reynolds, K.H. Drexhage, *Opt. Commun.* 13 (1975) 222–225;
- H. Zollinger, *Color Chemistry*, 3rd ed., Verlag Helvetica Chimica Acta: Zurich and Wiley-VCH, Weinheim, 2003;
- e) E.R. Bissell, A.R. Mitchell, R.E. Smith, *J. Org. Chem.* 45 (1980) 2283–2287;
- G.P. Ellis, *The Chemistry of Heterocyclic Compounds, Chromenes, Chromanones, and Chromones*, Eds., John Wiley, New York, NY (1977) 11–13 (Chapter II).
- [29] M. Khoobi, L. Ma'mani, F. Rezazadeh, Z. Zareie, A. Foroumadi, A. Ramazani, A. Shafiee, *J. Mol. Catal. A: Chem.* 359 (2012) 74–80.
- [30] B. Mu, P. Liu, Y. Dong, Ch. Lu, X. Wu, *J. Polym. Sci. Part A: Polym. Chem.* 48 (2010) 3135–3144.
- [31] D. Zois, C. Vartzouma, Y. Deligiannakis, N. Hadjiliadis, L. Casella, E. Monzani, M. Loulodi, *J. Mol. Catal. A: Chem.* 261 (2007) 306–317.
- [32] D. Fang, H.B. Zhang, Z.L. Liu, *J. Heterocycl. Chem.* 47 (2010) 63–67.
- [33] H.R. Shaterian, M. Arman, F. Rigi, *J. Mol. Liq.* 158 (2011) 145–150.
- [34] D. Kumar, V.B. Reddy, B.G. Mishra, R.K. Rana, M.N. Nadagouda, R.S. Varma, *Tetrahedron* 63 (2007) 3093–3097.
- [35] J.M. Khurana, B. Nand, P. Saluja, *Tetrahedron* 66 (2010) 5637–5641.
- [36] J.M. Khurana, S. Kumar, *Tetrahedron Lett.* 50 (2009) 4125–4127.
- [37] M. Mahdavi, A. Asadipour, S. Rajabalian, M. Vosooghi, L. Firoozpour, M. Nakhjiri, A. Shafiee, A. Foroumadi, E.-J. Chem. 8 (2011) 598.
- [38] H. Zeng, Q. Lai, X. Liu, D. Wen, X. Ji, *J. Appl. Polym. Sci.* 106 (2007) 3474.
- [39] O.u. Rahman, S. Ch. Mohapatra, Sh. Ahmad, *Mater. Chem. Phys.* 132 (2012) 196–202.